

An energy-based coupling approach to nonlocal interface problems

Giacomo Capodaglio², Marta D'Elia¹, Pavel Bochev¹, Max Gunzburger²

Abstract

Nonlocal models provide accurate representations of physical phenomena ranging from fracture mechanics to complex subsurface flows, where traditional partial differential equations fail to capture effects caused by long-range forces at the microscale and mesoscale. However, the application of nonlocal models to problems involving interfaces such as multimaterial simulations and fluid-structure interaction, is hampered by the lack of a rigorous nonlocal interface theory needed to support numerical developments. In this paper, we use an energy-based approach to develop a mathematically rigorous nonlocal interface theory which provides a physically consistent extension of the classical perfect interface PDE formulation. Numerical examples validate the proposed framework and demonstrate the scope of our theory.

Keywords: Nonlocal Models, Interface Problems, Heterogeneous Materials.

1. Introduction

Nonlocal models can accurately describe physical phenomena arising from long-range forces at the microscale and mesoscale. Such phenomena cannot be accounted for by partial differential equations (PDEs) where interaction is limited to points that are in direct contact with each other. As a result, mathematically nonlocal models are represented by integral operators, which are better suited to capture interactions occurring across a distance.

Examples of applications where long-range forces are essential for predictive simulations can be found in a diverse spectrum of scientific applications such as anomalous subsurface transport [1, 2, 3, 4], fracture mechanics [5, 6, 7], image processing [8, 9, 10, 11], magnetohydrodynamics [12], multiscale and multiphysics systems [13, 14], phase transitions [15, 16], and stochastic processes [17, 18, 19].

Although research on nonlocal models has recently intensified, there is still a lack of a mathematically rigorous and physically consistent nonlocal interface (NLI) theory. Examples of NLI research are few and far between in the literature with [20, 21] being perhaps the only published work in this field. However, the NLI formulations in these papers do not provide a rigorous theoretical framework because they do not address existence and uniqueness of solutions to NLI problems, nor do they establish formal convergence to local limits.

The absence of such a framework has hampered the wider adoption of nonlocal models in applications that require proper handling of material interfaces, such as multi-material simulations, fluid-structure interaction, and contact, to name a few. The main goal of this work is to fill this theoretical gap by providing a rigorous NLI theory that would establish a much needed foundation for the further development and application of nonlocal models in science and engineering applications.

¹Center for Computing Research, Sandia National Labs, e-mail: pbboche, mdelia@sandia.gov

²Department of Scientific Computing, Florida State University, e-mails: gcapodaglio, mgunzburger@fsu.edu

Nonlocal interface problems are challenging for a number of reasons rooted in the need to treat a local physical interface arising from material discontinuities in nonlocal terms. In particular, one of the key technical challenges is to discover appropriate nonlocal transmission conditions capable of providing physically consistent well-posed NLI problems that converge to classical formulations as the characteristic parameter of the nonlocal model goes to zero.

Our strategy is motivated by an energy-based description of classical local interface problems in which the local energy of the coupled system is minimized subject to constraints modeling the physics of the local interface. Here we follow this template to obtain mathematically rigorous NLI formulations by minimizing the nonlocal energy of the system subject to constraints describing the physics of the nonlocal interface. In so doing, we obtain nonlocal transmission conditions and well-posed NLI problems that converge to their local counterparts at the local limit.

The resulting mathematical NLI framework is validated through numerical experiments that confirm the theoretical predictions, provide additional insights on the NLI model and suggest follow-up research directions that will be pursued in forthcoming work.

The paper is structured as follows: in Section 2, we review a classical energy-based formulation of a local interface problem, which provides the template for its nonlocal counterpart. The fundamentals of nonlocal problems are highlighted in Section 3, where we introduce a nonlocal volume constrained problem. The nonlocal interface problem is introduced in Section 4, and local limits are derived in Section 5. Section 6 presents our numerical results.

2. Local interface problem

In this section, we review a classical energy-based formulation of local interface problems for second-order elliptic PDEs. Let Ω_1 and Ω_2 be two disjoint open and bounded subsets of \mathbb{R}^n , $n = 1, 2, 3$, with boundaries $\partial\Omega_1$ and $\partial\Omega_2$, respectively, and such that $\partial\Omega_1 \cap \partial\Omega_2 = \partial\Omega_2$.

Let $\Omega = \Omega_1 \cup \Omega_2$. The interface between the domains is denoted by Γ and is defined as $\Gamma = \partial\Omega_1 \cap \partial\Omega_2$. To facilitate the link between local and nonlocal interface problems, let us also set $\Gamma_1 = \partial\Omega_1 \setminus \Gamma$ and $\Gamma_2 = \partial\Omega_2 \setminus \Gamma$. Note that due to the configuration of the domains, $\Gamma_2 = \emptyset$ and $\Gamma = \partial\Omega_2$. Schematics of the domains for the local interface problem are given in Figure 1.

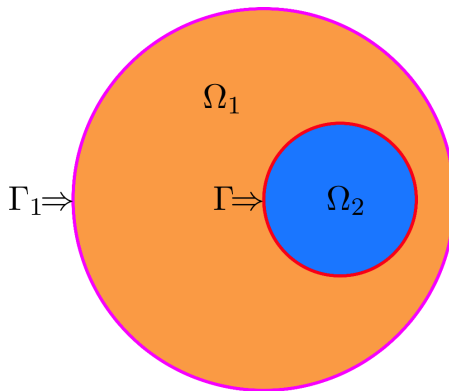


Figure 1: Illustration of the geometric configuration for the local interface problem.

2.1. Local energy minimization principle

Consider the following (local) energy functional

$$\begin{aligned} \mathcal{E}(u_1, u_2; f_1, f_2) = & \frac{1}{2} \int_{\Omega_1} \kappa_1(\mathbf{x}) |\nabla u_1(\mathbf{x})|^2 d\mathbf{x} - \int_{\Omega_1} f_1(\mathbf{x}) u_1(\mathbf{x}) d\mathbf{x} \\ & + \frac{1}{2} \int_{\Omega_2} \kappa_2(\mathbf{x}) |\nabla u_2(\mathbf{x})|^2 d\mathbf{x} - \int_{\Omega_2} f_2(\mathbf{x}) u_2(\mathbf{x}) d\mathbf{x}, \end{aligned} \quad (1)$$

where the functions κ_1 and κ_2 represent the different material properties of the two domains and are assumed to be positive and bounded from below. The functions f_1, f_2 are known.

We obtain a particular instance of a local interface problem by choosing a specific constrained minimization setting for (1). To this end, let us define the following energy spaces, for $i = 1, 2$

$$\begin{aligned} W_i = \{w \in H^1(\Omega_i) : |||w|||_i < \infty\}, \quad \text{where} \quad |||w|||_i = \sqrt{\|\nabla w\|_{0,\Omega_i}^2 + \|w\|_{0,\Omega_i}^2}, \\ W_i^c = \{w \in W_i : w(\mathbf{x}) = 0 \text{ on } \Gamma_i\}. \end{aligned} \quad (2)$$

Note that, due to the configuration of the domains depicted in Figure 1, $W_2^c = W_2$. Tensor product spaces are then defined as $W = W_1 \times W_2$ and $W^c = W_1^c \times W_2^c$.

Minimization Principle 2.1. *Given $g_1, g_2, f_1, f_2, \kappa_1$ and κ_2 , find $(u_1, u_2) \in W$ such that*

$$(u_1, u_2) = \arg \min_{(v_1, v_2) \in W} \mathcal{E}(v_1, v_2; f_1, f_2),$$

subject to the constraints

$$\begin{cases} u_1(\mathbf{x}) = g_1(\mathbf{x}) & \mathbf{x} \in \Gamma_1, \\ u_1(\mathbf{x}) = u_2(\mathbf{x}) & \mathbf{x} \in \Gamma. \end{cases} \quad (3)$$

The second constraint in (3), i.e., the continuity of the states across the interface, is a modeling assumption about the physics of the interface, which gives rise to a specific flavor of a local interface problem. This constraint is a particular case of a general coupling condition given by $u_1(\mathbf{x}) - \beta(\mathbf{x})u_2(\mathbf{x}) = \mu(\mathbf{x})$, where β and μ are some given functions. To avoid unnecessary technical details that are not essential for our purposes we do not consider this more general type of interface conditions in this paper.

2.2. Weak formulation

The Euler-Lagrange equation corresponding to the Minimization Principle 2.1 is given by the following weak variational equation: find $(u_1, u_2) \in W$ satisfying the constraints in (3) and such that

$$\int_{\Omega_1} \kappa_1(\mathbf{x}) \nabla u_1(\mathbf{x}) \cdot \nabla v_1(\mathbf{x}) d\mathbf{x} + \int_{\Omega_2} \kappa_2(\mathbf{x}) \nabla u_2(\mathbf{x}) \cdot \nabla v_2(\mathbf{x}) d\mathbf{x} = \int_{\Omega_1} f_1(\mathbf{x}) v_1(\mathbf{x}) d\mathbf{x} + \int_{\Omega_2} f_2(\mathbf{x}) v_2(\mathbf{x}) d\mathbf{x} \quad (4)$$

for all $(v_1, v_2) \in W^c$ satisfying $v_1(\mathbf{x}) = v_2(\mathbf{x})$ on Γ .

2.3. Strong formulation

As usual, we derive the strong form of the interface problem from the weak formulation (4) by assuming that u_1 and u_2 are sufficiently regular. Collecting terms, integrating by parts, and taking into account that $v_1 \in W^c$ yields

$$\begin{aligned} & \int_{\Omega_1} \left(-\nabla \cdot (\kappa_1(\mathbf{x}) \nabla u_1(\mathbf{x})) - f_1(\mathbf{x}) \right) v_1(\mathbf{x}) d\mathbf{x} + \int_{\Omega_2} \left(-\nabla \cdot (\kappa_2(\mathbf{x}) \nabla u_2(\mathbf{x})) - f_2(\mathbf{x}) \right) v_2(\mathbf{x}) d\mathbf{x} \\ & + \int_{\Gamma} v_1(\mathbf{x}) \kappa_1(\mathbf{x}) \nabla u_1(\mathbf{x}) \cdot \mathbf{n}_1 d\mathbf{x} + \int_{\Gamma} v_2(\mathbf{x}) \kappa_2(\mathbf{x}) \nabla u_2(\mathbf{x}) \cdot \mathbf{n}_2 d\mathbf{x} = 0. \end{aligned} \quad (5)$$

Because v_1 and v_2 are arbitrary on $\Omega_1 \cup \Gamma$ and $\Omega_2 \cup \Gamma$, respectively, we may first set v_1 arbitrary on Ω_1 , $v_1 = 0$ on Γ , and $v_2 = 0$ on $\Omega_2 \cup \Gamma$ and then set v_2 arbitrary on Ω_2 , $v_2 = 0$ on Γ , and $v_1 = 0$ on $\Omega_1 \cup \Gamma$ to obtain from (5) the strong forms $-\nabla \cdot (\kappa_i(\mathbf{x}) \nabla u_i(\mathbf{x})) = f_i(\mathbf{x})$ on Ω_i , $i = 1, 2$, of the subdomain equations. Substituting these equations back into (5) leaves us with

$$\int_{\Gamma} v_1(\mathbf{x}) \kappa_1(\mathbf{x}) \nabla u_1(\mathbf{x}) \cdot \mathbf{n}_1 d\mathbf{x} + \int_{\Gamma} v_2(\mathbf{x}) \kappa_2(\mathbf{x}) \nabla u_2(\mathbf{x}) \cdot \mathbf{n}_2 d\mathbf{x} = 0.$$

Using that $v_1 = v_2$ on Γ we then recover from this equation the *flux continuity condition* $\kappa_1(\mathbf{x}) \nabla u_1(\mathbf{x}) \cdot \mathbf{n}_1 + \kappa_2(\mathbf{x}) \nabla u_2(\mathbf{x}) \cdot \mathbf{n}_2 = 0$. Thus, the strong (PDE) form of the local interface problem corresponding to the Minimization Principle (2.1) is given by

$$-\nabla \cdot (\kappa_1(\mathbf{x}) \nabla u_1(\mathbf{x})) = f_1(\mathbf{x}) \quad \mathbf{x} \in \Omega_1, \quad (6)$$

$$u_1(\mathbf{x}) = g_1(\mathbf{x}) \quad \mathbf{x} \in \Gamma_1, \quad (7)$$

$$-\nabla \cdot (\kappa_2(\mathbf{x}) \nabla u_2(\mathbf{x})) = f_2(\mathbf{x}) \quad \mathbf{x} \in \Omega_2, \quad (8)$$

$$u_1(\mathbf{x}) = u_2(\mathbf{x}) \quad \mathbf{x} \in \Gamma, \quad (9)$$

$$\kappa_1(\mathbf{x}) \nabla u_1(\mathbf{x}) \cdot \mathbf{n}_1 + \kappa_2(\mathbf{x}) \nabla u_2(\mathbf{x}) \cdot \mathbf{n}_2 = 0 \quad \mathbf{x} \in \Gamma. \quad (10)$$

We note that the strong form of the interface problem contains the flux continuity condition (10) that was not explicitly present in Minimization Principle 1. This condition is a consequence of (9) that, as already mentioned, is a modeling assumption about the physics of the interface. Interfaces for which both the jumps in the state and in the normal flux are zero across the interface are known as *perfect interfaces* [22]. In contrast, interfaces for which one or both of these quantities are discontinuous across the interface are known as *imperfect*; see, e.g. [22].

3. Nonlocal volume constrained problems

In this section, we review the fundamentals of nonlocal volume constrained problems. Let Ω be an open and bounded subset of \mathbb{R}^n . Given a positive real number δ , we define the interaction domain $\tilde{\Gamma}$ associated with Ω as follows

$$\tilde{\Gamma} = \{\mathbf{y} \in \mathbb{R}^n \setminus \Omega : |\mathbf{x} - \mathbf{y}| \leq \delta, \text{ for } \mathbf{x} \in \Omega\}. \quad (11)$$

Note that $\tilde{\Gamma}$ depends on δ , even though it is not written explicitly. Figure 2 shows an example of a two-dimensional domain and its interaction region.

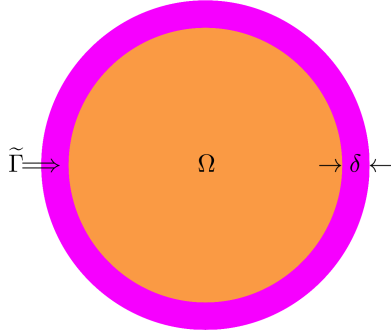


Figure 2: Illustration of the geometric configuration for the nonlocal volume-constrained problem.

3.1. Nonlocal energy minimization principle

In this work we use an energy-based characterization of nonlocal volume constrained problems which mirrors the Dirichlet principle for the gradient operator. Specifically, we seek the states of the nonlocal model as suitably constrained minimizers of the following nonlocal energy functional:

$$\mathcal{E}(u; \gamma, f) = \frac{1}{2} \int_{\Omega \cup \tilde{\Gamma}} \int_{\Omega \cup \tilde{\Gamma}} |u(\mathbf{y}) - u(\mathbf{x})|^2 \gamma(\mathbf{x}, \mathbf{y}) d\mathbf{y} d\mathbf{x} - \int_{\Omega} f(\mathbf{x}) u(\mathbf{x}) d\mathbf{x}. \quad (12)$$

The function γ is referred to as the *kernel* and is required to satisfy

$$\gamma(\mathbf{x}, \mathbf{y}) = \gamma(\mathbf{y}, \mathbf{x}), \quad \text{for } \mathbf{x}, \mathbf{y} \in \Omega \cup \tilde{\Gamma}. \quad (13)$$

Let us define the following function spaces

$$\begin{aligned} W &= \{v \in L^2(\Omega \cup \tilde{\Gamma}) : |||w||| < \infty\}, \\ \text{where } |||w|||^2 &= \int_{\Omega \cup \tilde{\Gamma}} \int_{\Omega \cup \tilde{\Gamma}} |w(\mathbf{y}) - w(\mathbf{x})|^2 \gamma(\mathbf{x}, \mathbf{y}) d\mathbf{y} d\mathbf{x} + \|w\|_{L^2(\Omega \cup \tilde{\Gamma})}^2, \\ W^c &= \{w \in W : w = 0 \text{ for } \mathbf{x} \in \tilde{\Gamma}\}. \end{aligned} \quad (14)$$

Minimization Principle 3.1. *Given γ , f , and g , find $u \in W$ such that*

$$u = \arg \min_{v \in W} \mathcal{E}(v; \gamma, f),$$

subject to $u(\mathbf{x}) = g(\mathbf{x})$ on $\tilde{\Gamma}$.

We refer to the constraint in the Minimization Principle 3.1 as a Dirichlet volume constraint because it generalizes the standard (local) Dirichlet boundary condition.

3.2. Weak formulation

The necessary optimality condition of the Minimization Principle 3.1 is given by the following variational equation: find $u \in W$ such that $u(\mathbf{x}) = g(\mathbf{x})$ on $\tilde{\Gamma}$ and

$$\int_{\Omega \cup \tilde{\Gamma}} \int_{\Omega \cup \tilde{\Gamma}} (v(\mathbf{y}) - v(\mathbf{x}))(u(\mathbf{y}) - u(\mathbf{x})) \gamma(\mathbf{x}, \mathbf{y}) d\mathbf{y} d\mathbf{x} = \int_{\Omega} v(\mathbf{x}) f(\mathbf{x}) d\mathbf{x} \quad (15)$$

for all $v \in W^c$.

3.3. Strong formulation

To state the strong form of (15) we recall the nonlocal diffusion operator

$$\mathcal{L}u(\mathbf{x}) = 2 \int_{\Omega \cup \tilde{\Gamma}} (u(\mathbf{y}) - u(\mathbf{x})) \gamma(\mathbf{x}, \mathbf{y}) d\mathbf{y}. \quad (16)$$

and the nonlocal Green's identity [23]

$$\begin{aligned} \int_{\Omega} v(\mathbf{x}) \mathcal{L}u(\mathbf{x}) d\mathbf{x} &= - \int_{\Omega \cup \tilde{\Gamma}} \int_{\Omega \cup \tilde{\Gamma}} (v(\mathbf{y}) - v(\mathbf{x})) (u(\mathbf{y}) - u(\mathbf{x})) \gamma(\mathbf{x}, \mathbf{y}) d\mathbf{y} d\mathbf{x} \\ &\quad - 2 \int_{\tilde{\Gamma}} \int_{\Omega \cup \tilde{\Gamma}} v(\mathbf{x}) (u(\mathbf{y}) - u(\mathbf{x})) \gamma(\mathbf{x}, \mathbf{y}) d\mathbf{y} d\mathbf{x}. \end{aligned} \quad (17)$$

Using (17) and the fact that $v = 0$ on $\tilde{\Gamma}$ one can transform (15) into the following equation

$$\int_{\Omega} v(\mathbf{x}) \mathcal{L}u(\mathbf{x}) d\mathbf{x} + \int_{\Omega} v(\mathbf{x}) f(\mathbf{x}) d\mathbf{x} = 0. \quad (18)$$

Since v is arbitrary on Ω one then easily obtains the strong form of the nonlocal volume constrained problem

$$\begin{aligned} -\mathcal{L}u(\mathbf{x}) &= f(\mathbf{x}) & \mathbf{x} \in \Omega \\ u(\mathbf{x}) &= g(\mathbf{x}) & \mathbf{x} \in \tilde{\Gamma}. \end{aligned} \quad (19)$$

4. Nonlocal interface problem

In this section we derive a mathematically rigorous formulation of a nonlocal interface problem that provides a physically consistent extension of the perfect local interface problem in Section 2. This nonlocal counterpart of a perfect interface problem represents the main contribution of the present work.

We retain the domain configuration from Section 2, i.e., Ω_1 and Ω_2 are disjoint bounded subsets of \mathbb{R}^n such that $\partial\Omega_1 \cap \partial\Omega_2 = \partial\Omega_2$, and $\Omega = \Omega_1 \cup \Omega_2$. In the nonlocal interface problem, the domains Ω_i interact with each other through regions that have nonzero measure. These regions are defined in different ways depending on the relative location of \mathbf{x} and \mathbf{y} and on two parameters δ_1 and δ_2 . Specifically, for $\delta_1 > 0$ and $\delta_2 > 0$, we introduce:

- $\Gamma_1 = \{\mathbf{y} \in \mathbb{R}^n \setminus \Omega_1 : |\mathbf{x} - \mathbf{y}| \leq \delta_1, \text{ for } \mathbf{x} \in \Omega_1\}$: the (external) interaction domain of Ω_1 .
- $\Gamma_{12} = \{\mathbf{y} \in \Omega_2 : |\mathbf{x} - \mathbf{y}| \leq \delta_1, \text{ for } \mathbf{x} \in \Omega_1\}$: the region of Ω_2 that interacts with Ω_1 when $\mathbf{x} \in \Omega_1$.
- $\Gamma_{21} = \{\mathbf{y} \in \Omega_1 : |\mathbf{x} - \mathbf{y}| \leq \delta_2, \text{ for } \mathbf{x} \in \Omega_2\}$: the region of Ω_1 that interacts with Ω_2 when $\mathbf{x} \in \Omega_2$.
- $\underline{\Gamma}_{12} = \{\mathbf{y} \in \Omega_2 : |\mathbf{x} - \mathbf{y}| \leq \delta_2, \text{ for } \mathbf{x} \in \Omega_1\}$: the analogue of Γ_{21} on Ω_2 .
- $\underline{\Gamma}_{21} = \{\mathbf{y} \in \Omega_1 : |\mathbf{x} - \mathbf{y}| \leq \delta_1, \text{ for } \mathbf{x} \in \Omega_2\}$: the analogue of Γ_{12} on Ω_1 .

Figures 3, 4, and 5 illustrate the geometric configuration for the nonlocal interface problem and the various subdomains involved. We also introduce the set $\Gamma^* = \Gamma_{ij} \cup \underline{\Gamma}_{ji}$ if $\delta_i \geq \delta_j$. Note that by definition $\Gamma_{ij} \subset \Gamma^*$

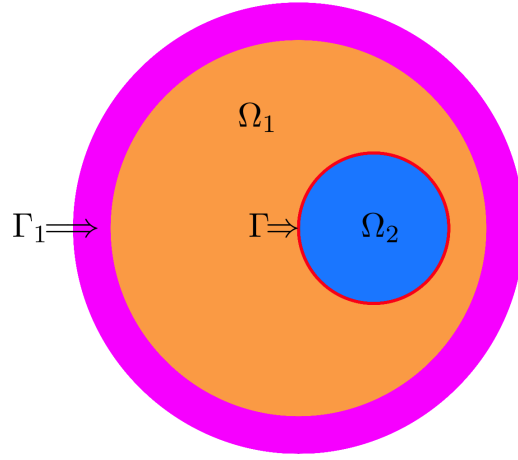


Figure 3: Illustration of the geometric configuration for the nonlocal interface problem.

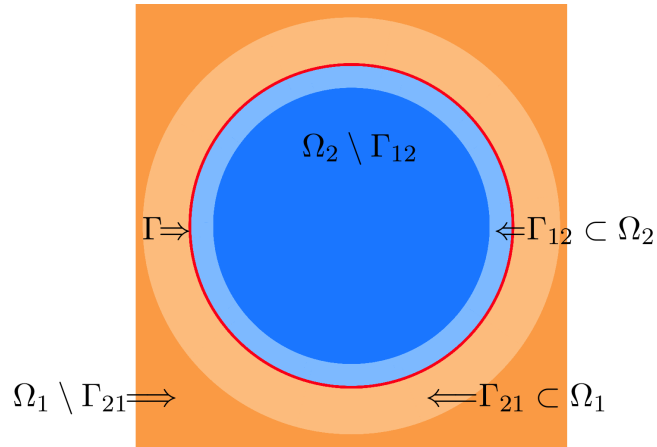


Figure 4: Illustration of the subdomains Γ_{12} and Γ_{21} .

and $\underline{\Gamma}_{ij} \subset \Gamma^*$ for any i and j . The kernel function γ is defined for all $(\mathbf{x}, \mathbf{y}) \in (\Omega_1 \cup \Gamma_1) \times (\Omega_1 \cup \Gamma_1)$ as follows:

$$\gamma(\mathbf{x}, \mathbf{y}) = \begin{cases} \gamma_{11}(\mathbf{x}, \mathbf{y}) = C_{11}(\delta_1) \mathcal{X}_{B_1(\mathbf{x})}(\mathbf{y}) & \mathbf{x} \in \Omega_1 \cup \Gamma_1, \mathbf{y} \in \Omega_1 \cup \Gamma_1 \\ \gamma_{12}(\mathbf{x}, \mathbf{y}) = C_{12}(\delta_1) \mathcal{X}_{B_1(\mathbf{x})}(\mathbf{y}) & \mathbf{x} \in \Omega_1 \cup \Gamma_1, \mathbf{y} \in \Omega_2 \\ \gamma_{21}(\mathbf{x}, \mathbf{y}) = C_{21}(\delta_2) \mathcal{X}_{B_2(\mathbf{x})}(\mathbf{y}) & \mathbf{x} \in \Omega_2, \mathbf{y} \in \Omega_1 \cup \Gamma_1 \\ \gamma_{22}(\mathbf{x}, \mathbf{y}) = C_{22}(\delta_2) \mathcal{X}_{B_2(\mathbf{x})}(\mathbf{y}) & \mathbf{x} \in \Omega_2, \mathbf{y} \in \Omega_2, \end{cases} \quad (20)$$

where \mathcal{X}_S is the indicator function on the set S . Examples of explicit definitions for the functions $C_{ij}(\delta_i)$ will be given in the local limits analysis.

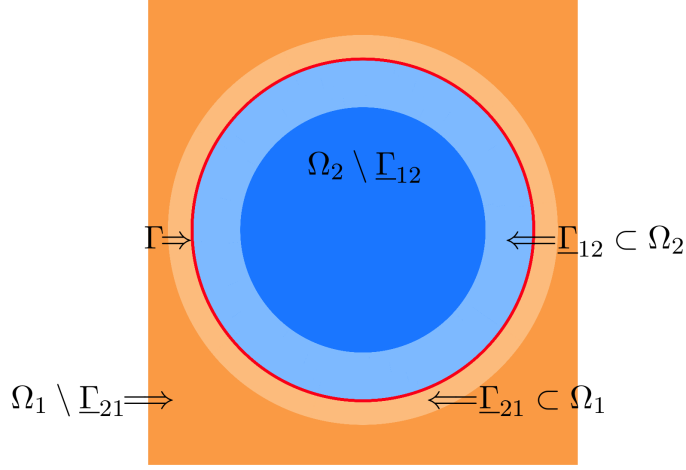


Figure 5: Illustration of the subdomains $\underline{\Gamma}_{12}$ and $\underline{\Gamma}_{21}$.

4.1. Nonlocal energy minimization principle

Following the energy-based description of the local perfect interface problem we start with defining the nonlocal energy of the system as follows

$$\mathcal{E}(u; \gamma, f) = \frac{1}{2} \int_{\Omega \cup \Gamma_1} \int_{\Omega \cup \Gamma_1} (u(\mathbf{x}) - u(\mathbf{y}))^2 \gamma(\mathbf{x}, \mathbf{y}) d\mathbf{y} d\mathbf{x} - \int_{\Omega} f(\mathbf{x}) u(\mathbf{x}) d\mathbf{x} \quad (21)$$

Using that Ω_1 and Ω_2 are disjoint, we split the energy in two parts, associating the first to u_1 and the second to u_2 , i.e.

$$\begin{aligned} \mathcal{E}_s(u_1, u_2; \gamma, f) &= \frac{1}{2} \int_{\Omega_1 \cup \Gamma_1} \int_{\Omega_1 \cup \Gamma_1} (u_1(\mathbf{x}) - u_1(\mathbf{y}))^2 \gamma(\mathbf{x}, \mathbf{y}) d\mathbf{y} d\mathbf{x} - \int_{\Omega_1} f u_1 d\mathbf{x} \\ &+ \frac{1}{2} \int_{\Omega_2} \int_{\Omega_1 \cup \Gamma_1} (u_2(\mathbf{x}) - u_2(\mathbf{y}))^2 \gamma(\mathbf{x}, \mathbf{y}) d\mathbf{y} d\mathbf{x} - \int_{\Omega_2} f u_2 d\mathbf{x}. \end{aligned} \quad (22)$$

Let us define the following function spaces

$$\begin{aligned} W_1 &= \{w \in L^2(\Omega_1 \cup \Gamma_1) : \|w\|_1^2 + \|w\|_{L^2(\Omega_1 \cup \Gamma_1)}^2 < \infty\}, \\ \text{where } \|w\|_1^2 &= \frac{1}{2} \int_{\Omega_1 \cup \Gamma_1} \int_{\Omega_1 \cup \Gamma_1} |u_1(\mathbf{y}) - u_1(\mathbf{x})|^2 \gamma_{11}(\mathbf{x}, \mathbf{y}) d\mathbf{y} d\mathbf{x}, \\ W_2 &= \{w \in L^2(\Omega_2) : \|w\|_2^2 + \|w\|_{L^2(\Omega_2)}^2 < \infty\}, \\ \text{where } \|w\|_2^2 &= \frac{1}{2} \int_{\Omega_2} \int_{\Omega_2} |u_2(\mathbf{y}) - u_2(\mathbf{x})|^2 \gamma_{22}(\mathbf{x}, \mathbf{y}) d\mathbf{y} d\mathbf{x}. \end{aligned} \quad (23)$$

The constrained space W_1^c is defined as

$$W_1^c = \{w \in W_1 : w(\mathbf{x}) = 0 \text{ on } \Gamma_1\}. \quad (24)$$

We also introduce the tensor product spaces $W = W_1 \times W_2$ and $W^c = W_1^c \times W_2$.

Minimization Principle 4.1. Given γ , and f , find $(u_1, u_2) \in W$ such that

$$(u_1, u_2) = \arg \min_{(v_1, v_2) \in W} \mathcal{E}(v_1, v_2; \gamma, f),$$

subject to the constraints

$$\begin{cases} u_1(\mathbf{x}) = g_1(\mathbf{x}) & \mathbf{x} \in \Gamma_1, \\ u_1(\mathbf{x}) = u_2(\mathbf{x}) & \mathbf{x} \in \Gamma^*. \end{cases} \quad (25)$$

The second constraint in (25) can be viewed as a generalization of the state continuity constraint in (3) much like the volume constraint in (19) generalizes the standard Dirichlet boundary condition.

4.2. Weak formulation

The Euler-Lagrange equation corresponding to the Minimization Principle 4.1 is given by the following weak variational equation: find $(u_1, u_2) \in W$ satisfying the constraints in (25) and such that

$$\begin{aligned} & \int_{\Omega_1 \cup \Gamma_1} \int_{\Omega_1 \cup \Gamma_1} (u_1(\mathbf{x}) - u_1(\mathbf{y}))(v_1(\mathbf{x}) - v_1(\mathbf{y}))\gamma(\mathbf{x}, \mathbf{y}) d\mathbf{y} d\mathbf{x} \\ & + \int_{\Omega_1 \cup \Gamma_1} \int_{\Omega_2} (u_1(\mathbf{x}) - u_1(\mathbf{y}))(v_1(\mathbf{x}) - v_1(\mathbf{y}))\gamma(\mathbf{x}, \mathbf{y}) d\mathbf{y} d\mathbf{x} - \int_{\Omega_1} f v_1 d\mathbf{x} \\ & + \int_{\Omega_2} \int_{\Omega_2} (u_2(\mathbf{x}) - u_2(\mathbf{y}))(v_2(\mathbf{x}) - v_2(\mathbf{y}))\gamma(\mathbf{x}, \mathbf{y}) d\mathbf{y} d\mathbf{x} \\ & + \int_{\Omega_2} \int_{\Omega_1 \cup \Gamma_1} (u_2(\mathbf{x}) - u_2(\mathbf{y}))(v_2(\mathbf{x}) - v_2(\mathbf{y}))\gamma(\mathbf{x}, \mathbf{y}) d\mathbf{y} d\mathbf{x} - \int_{\Omega_2} f v_2 d\mathbf{x} = 0, \end{aligned} \quad (26)$$

for all $(v_1, v_2) \in W^c$ satisfying $v_1(\mathbf{x}) = v_2(\mathbf{x})$ for $\mathbf{x} \in \Gamma^*$.

4.3. Strong formulation

The strong form of the nonlocal interface problem can be obtained from the weak form as follows. We begin by denoting the double integral terms in (26) by A , B , C , D and E , respectively, so that the weak equation assumes the form

$$A + B - \int_{\Omega_1} f v_1 d\mathbf{x} + C + D - \int_{\Omega_2} f v_2 d\mathbf{x} = 0. \quad (27)$$

To transform these terms we will use the following identity

$$\int_{D_1} \int_{D_2} \psi(\mathbf{x}, \mathbf{y})\sigma(\mathbf{y})\gamma(\mathbf{x}, \mathbf{y})d\mathbf{y}d\mathbf{x} = \int_{D_2} \sigma(\mathbf{x}) \int_{D_1} \psi(\mathbf{y}, \mathbf{x})\gamma(\mathbf{y}, \mathbf{x})d\mathbf{y}d\mathbf{x}, \quad (28)$$

where D_1 and D_2 are two generic subsets of \mathbb{R}^n . For the first term in equation (27), using that $v_1 = 0$ on Γ_1 , we have

$$\begin{aligned}
A &= \int_{\Omega_1 \cup \Gamma_1} v_1(\mathbf{x}) \int_{\Omega_1 \cup \Gamma_1} (u_1(\mathbf{x}) - u_1(\mathbf{y})) \gamma(\mathbf{x}, \mathbf{y}) d\mathbf{y} d\mathbf{x} - \int_{\Omega_1 \cup \Gamma_1} \int_{\Omega_1 \cup \Gamma_1} (u_1(\mathbf{x}) - u_1(\mathbf{y})) v_1(\mathbf{y}) \gamma(\mathbf{x}, \mathbf{y}) d\mathbf{y} d\mathbf{x} \\
&= \int_{\Omega_1} v_1(\mathbf{x}) \int_{\Omega_1 \cup \Gamma_1} (u_1(\mathbf{x}) - u_1(\mathbf{y})) \gamma(\mathbf{x}, \mathbf{y}) d\mathbf{y} d\mathbf{x} - \int_{\Omega_1 \cup \Gamma_1} v_1(\mathbf{x}) \int_{\Omega_1 \cup \Gamma_1} (u_1(\mathbf{y}) - u_1(\mathbf{x})) \gamma(\mathbf{y}, \mathbf{x}) d\mathbf{y} d\mathbf{x} \\
&= -2 \int_{\Omega_1} v_1(\mathbf{x}) \int_{\Omega_1 \cup \Gamma_1} (u_1(\mathbf{y}) - u_1(\mathbf{x})) \gamma_{11}(\mathbf{x}, \mathbf{y}) d\mathbf{y} d\mathbf{x}.
\end{aligned} \tag{29}$$

For B , we use again that $v_1 = 0$ on Γ_1 to obtain:

$$\begin{aligned}
B &= \int_{\Omega_1 \cup \Gamma_1} v_1(\mathbf{x}) \int_{\Omega_2} (u_1(\mathbf{x}) - u_1(\mathbf{y})) \gamma(\mathbf{x}, \mathbf{y}) d\mathbf{y} d\mathbf{x} - \int_{\Omega_1 \cup \Gamma_1} \int_{\Omega_2} (u_1(\mathbf{x}) - u_1(\mathbf{y})) v_1(\mathbf{y}) \gamma(\mathbf{x}, \mathbf{y}) d\mathbf{y} d\mathbf{x} \\
&= \int_{\Omega_1} v_1(\mathbf{x}) \int_{\Omega_2} (u_1(\mathbf{x}) - u_1(\mathbf{y})) \gamma(\mathbf{x}, \mathbf{y}) d\mathbf{y} d\mathbf{x} - \int_{\Omega_2} v_1(\mathbf{x}) \int_{\Omega_1 \cup \Gamma_1} (u_1(\mathbf{y}) - u_1(\mathbf{x})) \gamma(\mathbf{y}, \mathbf{x}) d\mathbf{y} d\mathbf{x} \\
&= \int_{\Omega_1} v_1(\mathbf{x}) \int_{\Omega_2} (u_1(\mathbf{x}) - u_1(\mathbf{y})) \gamma_{12}(\mathbf{x}, \mathbf{y}) d\mathbf{y} d\mathbf{x} - \int_{\Omega_2} v_1(\mathbf{x}) \int_{\Omega_1 \cup \Gamma_1} (u_1(\mathbf{y}) - u_1(\mathbf{x})) \gamma_{12}(\mathbf{y}, \mathbf{x}) d\mathbf{y} d\mathbf{x} \\
&= \int_{\Omega_1} v_1(\mathbf{x}) \int_{\Gamma_{12}} (u_1(\mathbf{x}) - u_2(\mathbf{y})) \gamma_{12}(\mathbf{x}, \mathbf{y}) d\mathbf{y} d\mathbf{x} - \int_{\Omega_2} v_2(\mathbf{x}) \int_{\underline{\Gamma}_{21}} (u_1(\mathbf{y}) - u_2(\mathbf{x})) \gamma_{12}(\mathbf{x}, \mathbf{y}) d\mathbf{y} d\mathbf{x}.
\end{aligned} \tag{30}$$

A few comments on the last equality: in the first term we used that $u_1 = u_2$ on Γ_{12} , whereas in the second term the outer integral is non-zero only on Γ_{12} , thus we used the condition $v_1 = v_2$ on Γ_{12} . Note that the inner integral in the second term is non-zero only on $\underline{\Gamma}_{21}$, because the region of influence is determined a ball of radius δ_1 , from the definition of γ_{12} . Again in the second term, used the fact that $u_1 = u_2$ on Γ_{12} and substituted $u_1(\mathbf{x})$ with $u_2(\mathbf{x})$ in the inner integral. For the term labeled C in equation (27) we use the same reasoning as for A and obtain:

$$\begin{aligned}
C &= \int_{\Omega_2} v_2(\mathbf{x}) \int_{\Omega_2} (u_2(\mathbf{x}) - u_2(\mathbf{y})) \gamma(\mathbf{x}, \mathbf{y}) d\mathbf{y} d\mathbf{x} - \int_{\Omega_2} \int_{\Omega_2} (u_2(\mathbf{x}) - u_2(\mathbf{y})) v_2(\mathbf{y}) \gamma(\mathbf{x}, \mathbf{y}) d\mathbf{y} d\mathbf{x} \\
&= \int_{\Omega_2} v_2(\mathbf{x}) \int_{\Omega_2} (u_2(\mathbf{x}) - u_2(\mathbf{y})) \gamma(\mathbf{x}, \mathbf{y}) d\mathbf{y} d\mathbf{x} - \int_{\Omega_2} v_2(\mathbf{x}) \int_{\Omega_2} (u_2(\mathbf{y}) - u_2(\mathbf{x})) \gamma(\mathbf{y}, \mathbf{x})(\mathbf{x}, \mathbf{y}) d\mathbf{y} d\mathbf{x} \\
&= -2 \int_{\Omega_2} v_2(\mathbf{x}) \int_{\Omega_2} (u_2(\mathbf{y}) - u_2(\mathbf{x})) \gamma_{22}(\mathbf{x}, \mathbf{y}) d\mathbf{y} d\mathbf{x}.
\end{aligned} \tag{31}$$

For the last term in equation (27), labeled D , we proceed as for B to get:

$$\begin{aligned}
D &= \int_{\Omega_2} v_2(\mathbf{x}) \int_{\Omega_1 \cup \Gamma_1} (u_2(\mathbf{x}) - u_2(\mathbf{y})) \gamma(\mathbf{x}, \mathbf{y}) d\mathbf{y} d\mathbf{x} - \int_{\Omega_2} \int_{\Omega_1 \cup \Gamma_1} (u_2(\mathbf{x}) - u_2(\mathbf{y})) v_2(\mathbf{y}) \gamma(\mathbf{x}, \mathbf{y}) d\mathbf{y} d\mathbf{x} \\
&= \int_{\Omega_2} v_2(\mathbf{x}) \int_{\Omega_1 \cup \Gamma_1} (u_2(\mathbf{x}) - u_2(\mathbf{y})) \gamma_{21}(\mathbf{x}, \mathbf{y}) d\mathbf{y} d\mathbf{x} - \int_{\Omega_1 \cup \Gamma_1} v_2(\mathbf{x}) \int_{\Omega_2} (u_2(\mathbf{y}) - u_2(\mathbf{x})) \gamma(\mathbf{y}, \mathbf{x}) d\mathbf{y} d\mathbf{x} \\
&= \int_{\Omega_2} v_2(\mathbf{x}) \int_{\Gamma_{21}} (u_2(\mathbf{x}) - u_1(\mathbf{y})) \gamma_{21}(\mathbf{x}, \mathbf{y}) d\mathbf{y} d\mathbf{x} - \int_{\Omega_1 \cup \Gamma_1} v_2(\mathbf{x}) \int_{\Omega_2} (u_2(\mathbf{y}) - u_2(\mathbf{x})) \gamma_{21}(\mathbf{y}, \mathbf{x}) d\mathbf{y} d\mathbf{x} \\
&= \int_{\Omega_2} v_2(\mathbf{x}) \int_{\Gamma_{21}} (u_2(\mathbf{x}) - u_1(\mathbf{y})) \gamma_{21}(\mathbf{x}, \mathbf{y}) d\mathbf{y} d\mathbf{x} - \int_{\Omega_1} v_1(\mathbf{x}) \int_{\Gamma_{12}} (u_2(\mathbf{y}) - u_1(\mathbf{x})) \gamma_{21}(\mathbf{x}, \mathbf{y}) d\mathbf{y} d\mathbf{x}.
\end{aligned} \tag{32}$$

To obtain the strong form of the nonlocal interface problem, we now collect all contributions from A , B , C and D and exploit the fact that v_1 and v_2 are independent of each other and arbitrary in Ω_1 and Ω_2 . The resulting nonlocal subdomain problems are given by

$$\left. \begin{aligned}
&-2 \int_{\Omega_1 \cup \Gamma_1} (u_1(\mathbf{y}) - u_1(\mathbf{x})) \gamma_{11}(\mathbf{x}, \mathbf{y}) d\mathbf{y} \\
&- \int_{\Gamma_{12}} (u_2(\mathbf{y}) - u_1(\mathbf{x})) \gamma_{12}(\mathbf{x}, \mathbf{y}) d\mathbf{y} \\
&- \int_{\Gamma_{12}} (u_2(\mathbf{y}) - u_1(\mathbf{x})) \gamma_{21}(\mathbf{x}, \mathbf{y}) d\mathbf{y} = f
\end{aligned} \right\} \mathbf{x} \in \Omega_1, \tag{33}$$

and

$$\left. \begin{aligned}
&-2 \int_{\Omega_2} (u_2(\mathbf{y}) - u_2(\mathbf{x})) \gamma_{22}(\mathbf{x}, \mathbf{y}) d\mathbf{y} \\
&- \int_{\Gamma_{21}} (u_1(\mathbf{y}) - u_2(\mathbf{x})) \gamma_{21}(\mathbf{x}, \mathbf{y}) d\mathbf{y} \\
&- \int_{\Gamma_{21}} (u_1(\mathbf{y}) - u_2(\mathbf{x})) \gamma_{12}(\mathbf{x}, \mathbf{y}) d\mathbf{y} = f
\end{aligned} \right\} \mathbf{x} \in \Omega_2. \tag{34}$$

respectively. Next, we isolate terms in (33) and (34) that do not interact with Ω_2 and Ω_1 respectively. After substituting (20), we obtain the following two equations:

$$\begin{aligned}
&-2 \int_{(\Omega_1 \cup \Gamma_1) \cap B_1(\mathbf{x})} (u_1(\mathbf{y}) - u_1(\mathbf{x})) C_{11}(\delta_1) d\mathbf{y} = f \quad \mathbf{x} \in \Omega_1 \setminus \Gamma_{21} \\
&-2 \int_{\Omega_2 \cap B_2(\mathbf{x})} (u_2(\mathbf{y}) - u_2(\mathbf{x})) C_{22}(\delta_2) d\mathbf{y} = f \quad \mathbf{x} \in \Omega_2 \setminus \Gamma_{12}
\end{aligned} \tag{35}$$

Collecting the remaining terms then yields

$$\begin{aligned}
& -2 \int_{(\Omega_1 \cup \Gamma_1) \cap B_1(\mathbf{x})} (u_1(\mathbf{y}) - u_1(\mathbf{x})) C_{11}(\delta_1) d\mathbf{y} \\
& - \int_{\Gamma_{12} \cap B_1(\mathbf{x})} (u_2(\mathbf{y}) - u_1(\mathbf{x})) C_{12}(\delta_1) d\mathbf{y} \\
& - \int_{\Gamma_{12} \cap B_2(\mathbf{x})} (u_2(\mathbf{y}) - u_1(\mathbf{x})) C_{21}(\delta_2) d\mathbf{y} = f \quad \mathbf{x} \in \underline{\Gamma}_{21}.
\end{aligned} \tag{36}$$

and

$$\begin{aligned}
& -2 \int_{\Omega_2 \cap B_2(\mathbf{x})} (u_2(\mathbf{y}) - u_2(\mathbf{x})) C_{22}(\delta_2) d\mathbf{y} \\
& - \int_{\Gamma_{21} \cap B_2(\mathbf{x})} (u_1(\mathbf{y}) - u_2(\mathbf{x})) C_{21}(\delta_2) d\mathbf{y} = \\
& - \int_{\Gamma_{21} \cap B_1(\mathbf{x})} (u_1(\mathbf{y}) - u_2(\mathbf{x})) C_{12}(\delta_1) d\mathbf{y} = f \quad \mathbf{x} \in \underline{\Gamma}_{12}.
\end{aligned} \tag{37}$$

respectively. We refer to these equations as the *nonlocal flux interface conditions*. To summarize, the strong form of the nonlocal interface problem comprises the subdomain equations (33) and (34), the volumetric constraints in (25), and nonlocal flux interface conditions (36) and (37). Together, these equations and interface conditions represent a nonlocal extension of the perfect interface PDE formulation (6)–(10).

5. Local limits of the interface conditions

In this section, we compute the local limits of the nonlocal interface conditions (36)–(37) and show that they converge to the local interface condition (10). We begin by showing that, in the local limit, the nonlocal diffusion operator (16) converges to the Laplace operator.

5.1. Convergence to the local operator

We want to show that

$$\lim_{\delta_i \rightarrow 0} \mathcal{L}(u_i) = -\kappa_i \Delta u_i, \quad i = 1, 2; \tag{38}$$

where κ_i is a positive constant and \mathcal{L}_i is the nonlocal diffusion operator (16) with kernel $\gamma = \gamma_{ii}$. To that end, let $\gamma_{ii}(\mathbf{x}, \mathbf{y}) = C_{ii}(\delta_i) \chi_{B_i(\mathbf{x})}(\mathbf{y}) = \tilde{C}_{ii} \delta_i^\beta \chi_{B_i(\mathbf{x})}(\mathbf{y})$, where \tilde{C}_{ii} is a positive constant and β is a positive integer, both to be determined. Assuming a smooth enough u_i , we use the following Taylor expansion

$$u_i(\mathbf{x}) - u_i(\mathbf{y}) = (\mathbf{x} - \mathbf{y}) \cdot \nabla u_i(\mathbf{x}) + \frac{1}{2} (\mathbf{x} - \mathbf{y}) \cdot (H_{u_i}(\mathbf{x}) \cdot (\mathbf{y} - \mathbf{x})) + \mathcal{O}(\delta_i^3), \tag{39}$$

where $H_{u_i}(\mathbf{x})$ is the Hessian matrix of u_i evaluated at \mathbf{x} . The nonlocal operator is therefore approximated by the following sum of integrals

$$\begin{aligned} & 2 \int_{B_i(\mathbf{x})} \tilde{C}_{ii} \delta_i^\beta (\mathbf{x} - \mathbf{y}) \cdot \nabla u_i(\mathbf{x}) d\mathbf{y} \\ & + \int_{B_i(\mathbf{x})} \tilde{C}_{ii} \delta_i^\beta (\mathbf{x} - \mathbf{y}) \cdot (H_{u_i}(\mathbf{x}) \cdot (\mathbf{y} - \mathbf{x})) d\mathbf{y} \\ & + \int_{B_i(\mathbf{x})} \tilde{C}_{ii} \delta_i^\beta \mathcal{O}(\delta_i^3) d\mathbf{y}. \end{aligned} \quad (40)$$

Without loss of generality, we have assumed that $\text{dist}(\mathbf{x}, \partial\Omega_i) > \delta_i$, in order to have $\Omega_i \cap B_i(\mathbf{x}) = B_i(\mathbf{x})$. Because with this assumption the integration is carried out over a ball, to compute the integrals we switch to polar coordinates. Letting $\mathbf{z} = \mathbf{y} - \mathbf{x}$ and $\rho = \|\mathbf{z}\|$, for the first integral we have

$$2 \int_{B_i(\mathbf{x})} \tilde{C}_{ii} \delta_i^\beta (\mathbf{x} - \mathbf{y}) \cdot \nabla u_i(\mathbf{x}) d\mathbf{y} = -2 \tilde{C}_{ii} \delta_i^\beta \int_{B_i(\mathbf{0})} \mathbf{z} \cdot \nabla u_i(\mathbf{x}) d\mathbf{z} = 0. \quad (41)$$

Before addressing the second integral, let us consider that

$$\begin{aligned} (\mathbf{x} - \mathbf{y}) \cdot (H_{u_i}(\mathbf{x}) \cdot (\mathbf{y} - \mathbf{x})) &= -\left(u_{xx}(\mathbf{x}) (x_1 - y_1)^2 + u_{xy}(\mathbf{x}) (x_1 - y_1) (x_2 - y_2) \right. \\ &\quad \left. + u_{yx}(\mathbf{x}) (x_2 - y_2) (x_1 - y_1) + u_{yy}(\mathbf{x}) (x_2 - y_2)^2 \right). \end{aligned} \quad (42)$$

Therefore, with the same change of variable as for the first integral, for the second integral we obtain

$$\begin{aligned} & \int_{B_i(\mathbf{x})} \tilde{C}_{ii} \delta_i^\beta (\mathbf{x} - \mathbf{y}) \cdot (H_{u_i}(\mathbf{x}) \cdot (\mathbf{y} - \mathbf{x})) d\mathbf{y} = - \int_{B_i(\mathbf{0})} \tilde{C}_{ii} \delta_i^\beta \mathbf{z} \cdot (H_{u_i}(\mathbf{x}) \cdot \mathbf{z}) d\mathbf{z} \\ & - u_{xx}(\mathbf{x}) \tilde{C}_{ii} \delta_i^\beta \int_0^{\delta_i} \rho^3 d\rho \int_0^{2\pi} \cos^2(\theta) d\theta - 2 u_{xy}(\mathbf{x}) \tilde{C}_{ii} \delta_i^\beta \int_0^{\delta_i} \rho^3 d\rho \int_0^{2\pi} \cos(\theta) \sin(\theta) d\theta \\ & - u_{yy}(\mathbf{x}) \tilde{C}_{ii} \delta_i^\beta \int_0^{\delta_i} \rho^3 d\rho \int_0^{2\pi} \sin^2(\theta) d\theta = -\left(\pi \tilde{C}_{ii} \delta_i^\beta \int_0^{\delta_i} \rho^3 d\rho \right) \Delta u_i. \end{aligned} \quad (43)$$

For the third integral we have

$$\int_{B_i(\mathbf{x})} \tilde{C}_{ii} \delta_i^\beta \mathcal{O}(\delta_i^3) d\mathbf{y} = 2\pi \tilde{C}_{ii} \delta_i^\beta \mathcal{O}(\delta_i^3) \int_0^{\delta_i} \rho d\rho. \quad (44)$$

Therefore, the following two conditions

$$\begin{aligned} & \lim_{\delta_i \rightarrow 0} \pi \tilde{C}_{ii} \delta_i^\beta \int_0^{\delta_i} \rho^3 d\rho = \kappa_i \\ & \lim_{\delta_i \rightarrow 0} 2\pi \tilde{C}_{ii} \delta_i^\beta \mathcal{O}(\delta_i^3) \int_0^{\delta_i} \rho d\rho = 0 \end{aligned} \quad (45)$$

are sufficient for (38) to hold. The second condition can be satisfied by setting $\beta = -4$ in which case the first condition yields

$$\tilde{C}_{ii} = \frac{4}{\pi} \kappa_i, \quad i = 1, 2. \quad (46)$$

Local limits of the interface conditions

In light of the analysis in the previous section, the kernel γ is defined as in equation (20), with

$$C_{ii}(\delta_i) = \frac{4\kappa_i}{\pi\delta_i^4}, \quad C_{ij}(\delta_i) = \frac{\tilde{C}_{ij}}{\delta_i^4}, \quad (47)$$

where \tilde{C}_{ij} is to be determined. Because we are considering $\delta_1 \rightarrow 0$ and $\delta_2 \rightarrow 0$, let us assume without loss of generality that $\mathbf{x} \in \Gamma$. For simplicity, we consider \mathbf{x} to be on the Ω_1 -side of Γ . The analysis would be similar assuming \mathbf{x} on a different side of Γ . Consider a reference frame (\mathbf{n}, \mathbf{t}) with origin on \mathbf{x} such that \mathbf{n} is the normal to Γ pointing inward towards Ω_2 and \mathbf{t} is a unit vector tangential to Γ and pointing up. Relative to this frame we have that $\mathbf{x} = \mathbf{0}$. With these assumptions we have, for $\mathbf{x} \in \underline{\Gamma}_{21}$

$$\begin{aligned} & -\frac{8\kappa_1}{\pi\delta_1^4} \int_{\underline{\Gamma}_{21} \cap B_1(\mathbf{0})} (u_1(\mathbf{y}) - u_1(\mathbf{0})) d\mathbf{y} - \frac{\tilde{C}_{12}}{\delta_1^4} \int_{\Gamma_{12} \cap B_1(\mathbf{0})} (u_2(\mathbf{y}) - u_1(\mathbf{0})) d\mathbf{y} \\ & - \frac{\tilde{C}_{21}}{\delta_2^4} \int_{\underline{\Gamma}_{12} \cap B_2(\mathbf{0})} (u_2(\mathbf{y}) - u_1(\mathbf{0})) d\mathbf{y} = f \end{aligned} \quad (48)$$

Using that $u_1 = u_2$ on Γ^* , with a Taylor expansion we get

$$\begin{aligned} & -\frac{8\kappa_1}{\pi\delta_1^4} \int_{\underline{\Gamma}_{21} \cap B_1(\mathbf{0})} (\mathbf{y} \cdot \mathbf{t}) (\mathbf{t} \cdot \nabla u_1(\mathbf{0})) d\mathbf{y} - \frac{8\kappa_1}{\pi\delta_1^4} \int_{\underline{\Gamma}_{21} \cap B_1(\mathbf{0})} (\mathbf{y} \cdot \mathbf{n}) (\mathbf{n} \cdot \nabla u_1(\mathbf{0})) d\mathbf{y} + \frac{1}{\delta_1^4} \int_{\underline{\Gamma}_{21} \cap B_1(\mathbf{0})} \mathcal{O}(\delta_1^2) d\mathbf{y} \\ & - \frac{\tilde{C}_{12}}{\delta_1^4} \int_{\Gamma_{12} \cap B_1(\mathbf{0})} (u_2(\mathbf{0}) - u_1(\mathbf{0})) d\mathbf{y} - \frac{\tilde{C}_{12}}{\delta_1^4} \int_{\Gamma_{12} \cap B_1(\mathbf{0})} (\mathbf{y} \cdot \mathbf{t}) (\mathbf{t} \cdot \nabla u_2(\mathbf{0})) d\mathbf{y} \\ & - \frac{\tilde{C}_{12}}{\delta_1^4} \int_{\Gamma_{12} \cap B_1(\mathbf{0})} (\mathbf{y} \cdot \mathbf{n}) (\mathbf{n} \cdot \nabla u_2(\mathbf{0})) d\mathbf{y} + \frac{1}{\delta_1^4} \int_{\Gamma_{12} \cap B_1(\mathbf{0})} \mathcal{O}(\delta_1^2) d\mathbf{y} \\ & - \frac{\tilde{C}_{21}}{\delta_2^4} \int_{\underline{\Gamma}_{12} \cap B_2(\mathbf{0})} (\mathbf{y} \cdot \mathbf{t}) (\mathbf{t} \cdot \nabla u_1(\mathbf{0})) d\mathbf{y} - \frac{\tilde{C}_{21}}{\delta_2^4} \int_{\underline{\Gamma}_{12} \cap B_2(\mathbf{0})} (\mathbf{y} \cdot \mathbf{n}) (\mathbf{n} \cdot \nabla u_1(\mathbf{0})) d\mathbf{y} \\ & + \frac{1}{\delta_2^4} \int_{\underline{\Gamma}_{12} \cap B_2(\mathbf{0})} \mathcal{O}(\delta_2^2) d\mathbf{y} = f. \end{aligned} \quad (49)$$

Converting to polar coordinates we get

$$\begin{aligned} & \frac{16\kappa_1}{\pi\delta_1^4} (\mathbf{n} \cdot \nabla u_1(\mathbf{0})) \int_0^{\delta_1} \rho^2 d\rho + \mathcal{O}(\delta_1^{-2}) \int_0^{\delta_1} \rho d\rho - \frac{\tilde{C}_{12}}{\delta_1^4} (u_2(\mathbf{0}) - u_1(\mathbf{0})) \pi \int_0^{\delta_1} \rho d\rho \\ & - \frac{2\tilde{C}_{12}}{\delta_1^4} (\mathbf{n} \cdot \nabla u_2(\mathbf{0})) \int_0^{\delta_1} \rho^2 d\rho - \frac{2\tilde{C}_{21}}{\delta_2^4} (\mathbf{n} \cdot \nabla u_1(\mathbf{0})) \int_0^{\delta_2} \rho^2 d\rho + \mathcal{O}(\delta_2^{-2}) \int_0^{\delta_2} \rho d\rho = f. \end{aligned} \quad (50)$$

We introduce conditions on \tilde{C}_{12} and \tilde{C}_{21} , namely

$$\tilde{C}_{12} = \frac{4\kappa_2}{\pi}, \quad \tilde{C}_{21} = \frac{4\kappa_1}{\pi}. \quad (51)$$

Using the above definition and computing integrals in $d\rho$ we get

$$\frac{16\kappa_1}{3\pi\delta_1} (\mathbf{n} \cdot \nabla u_1(\mathbf{0})) + \mathcal{O}(1) - \frac{2\kappa_2}{\delta_1^2} (u_2(\mathbf{0}) - u_1(\mathbf{0})) - \frac{8\kappa_2}{3\pi\delta_1} (\mathbf{n} \cdot \nabla u_2(\mathbf{0})) - \frac{8\kappa_1}{3\pi\delta_2} (\mathbf{n} \cdot \nabla u_1(\mathbf{0})) = f. \quad (52)$$

Multiplying equation (52) by δ_1^2 we obtain

$$\frac{16 \kappa_1 \delta_1}{3 \pi} \left(\mathbf{n} \cdot \nabla u_1(\mathbf{0}) \right) + \mathcal{O}(\delta_1^2) - 2 \kappa_2 (u_2(\mathbf{0}) - u_1(\mathbf{0})) - \frac{8 \kappa_2 \delta_1}{3 \pi} \left(\mathbf{n} \cdot \nabla u_2(\mathbf{0}) \right) - \frac{8 \kappa_1 \delta_1^2}{3 \pi \delta_2} \left(\mathbf{n} \cdot \nabla u_1(\mathbf{0}) \right) = \delta_1^2 f. \quad (53)$$

We now make an additional assumption on δ_1 and δ_2 , namely

$$\lim_{\delta_1 \rightarrow 0} \lim_{\delta_2 \rightarrow 0} \frac{\delta_1}{\delta_2} = 1. \quad (54)$$

The above equation holds true anytime there exists an $M > 0$ such that for each $\delta_1 < M$ and $\delta_2 < M$ we have $\delta_1 = \delta_2$. Hence, taking the limits in equation (53) we obtain

$$u_2(\mathbf{0}) = u_1(\mathbf{0}) \implies u_2(\mathbf{x}) = u_1(\mathbf{x}) \quad \text{on } \mathbf{x} \in \Gamma. \quad (55)$$

Multiplying equation (52) by δ_1 and taking limits we obtain

$$\frac{8 \kappa_1}{3 \pi} \left(\mathbf{n} \cdot \nabla u_1(\mathbf{0}) \right) - \frac{8 \kappa_2}{3 \pi} \left(\mathbf{n} \cdot \nabla u_2(\mathbf{0}) \right) = 0 \implies \kappa_1 \left(\mathbf{n} \cdot \nabla u_1(\mathbf{x}) \right) = \kappa_2 \left(\mathbf{n} \cdot \nabla u_2(\mathbf{x}) \right) \quad \text{on } \mathbf{x} \in \Gamma. \quad (56)$$

For $\mathbf{x} \in \underline{\Gamma}_{12}$, using equation (51) we have

$$\begin{aligned} & -\frac{8 \kappa_2}{\pi \delta_2^4} \int_{\underline{\Gamma}_{12} \cap B_2(\mathbf{0})} (u_2(\mathbf{y}) - u_2(\mathbf{0})) d\mathbf{y} - \frac{4 \kappa_1}{\pi \delta_2^4} \int_{\underline{\Gamma}_{21} \cap B_2(\mathbf{0})} (u_1(\mathbf{y}) - u_2(\mathbf{0})) d\mathbf{y} \\ & - \frac{4 \kappa_2}{\pi \delta_1^4} \int_{\underline{\Gamma}_{21} \cap B_1(\mathbf{0})} (u_1(\mathbf{y}) - u_2(\mathbf{0})) d\mathbf{y} = f \end{aligned} \quad (57)$$

Using that $u_1 = u_2$ on Γ^* , with a Taylor expansion we get

$$\begin{aligned} & -\frac{8 \kappa_2}{\pi \delta_2^4} \int_{\underline{\Gamma}_{12} \cap B_2(\mathbf{0})} (\mathbf{y} \cdot \mathbf{t}) \left(\mathbf{t} \cdot \nabla u_2(\mathbf{0}) \right) d\mathbf{y} - \frac{8 \kappa_2}{\pi \delta_2^4} \int_{\underline{\Gamma}_{12} \cap B_2(\mathbf{0})} (\mathbf{y} \cdot \mathbf{n}) \left(\mathbf{n} \cdot \nabla u_2(\mathbf{0}) \right) d\mathbf{y} + \frac{1}{\delta_2^4} \int_{\underline{\Gamma}_{12} \cap B_2(\mathbf{0})} \mathcal{O}(\delta_2^2) d\mathbf{y} \\ & - \frac{4 \kappa_1}{\pi \delta_2^4} \int_{\underline{\Gamma}_{21} \cap B_2(\mathbf{0})} (u_1(\mathbf{0}) - u_2(\mathbf{0})) d\mathbf{y} - \frac{4 \kappa_1}{\pi \delta_2^4} \int_{\underline{\Gamma}_{21} \cap B_2(\mathbf{0})} (\mathbf{y} \cdot \mathbf{t}) \left(\mathbf{t} \cdot \nabla u_1(\mathbf{0}) \right) d\mathbf{y} \\ & - \frac{4 \kappa_1}{\pi \delta_2^4} \int_{\underline{\Gamma}_{21} \cap B_2(\mathbf{0})} (\mathbf{y} \cdot \mathbf{n}) \left(\mathbf{n} \cdot \nabla u_1(\mathbf{0}) \right) d\mathbf{y} + \frac{1}{\delta_2^4} \int_{\underline{\Gamma}_{21} \cap B_2(\mathbf{0})} \mathcal{O}(\delta_2^2) d\mathbf{y} - \frac{4 \kappa_2}{\pi \delta_1^4} \int_{\underline{\Gamma}_{21} \cap B_1(\mathbf{0})} (\mathbf{y} \cdot \mathbf{t}) \left(\mathbf{t} \cdot \nabla u_2(\mathbf{0}) \right) d\mathbf{y} \\ & - \frac{4 \kappa_2}{\pi \delta_1^4} \int_{\underline{\Gamma}_{21} \cap B_1(\mathbf{0})} (\mathbf{y} \cdot \mathbf{n}) \left(\mathbf{n} \cdot \nabla u_2(\mathbf{0}) \right) d\mathbf{y} + \frac{1}{\delta_1^4} \int_{\underline{\Gamma}_{21} \cap B_1(\mathbf{0})} \mathcal{O}(\delta_1^2) d\mathbf{y} = f. \end{aligned} \quad (58)$$

Converting to polar coordinates we get

$$\begin{aligned} & -\frac{16 \kappa_2}{\pi \delta_2^4} \left(\mathbf{n} \cdot \nabla u_2(\mathbf{0}) \right) \int_0^{\delta_2} \rho^2 d\rho + \mathcal{O}(\delta_2^{-2}) \int_0^{\delta_2} \rho d\rho - \frac{4 \kappa_1}{\pi \delta_2^4} (u_1(\mathbf{0}) - u_2(\mathbf{0})) \pi \int_0^{\delta_2} \rho d\rho \\ & + \frac{8 \kappa_1}{\pi \delta_2^4} \left(\mathbf{n} \cdot \nabla u_1(\mathbf{0}) \right) \int_0^{\delta_2} \rho^2 d\rho + \frac{8 \kappa_2}{\pi \delta_1^4} \left(\mathbf{n} \cdot \nabla u_2(\mathbf{0}) \right) \int_0^{\delta_1} \rho^2 d\rho + \mathcal{O}(\delta_1^{-2}) \int_0^{\delta_1} \rho d\rho = f. \end{aligned} \quad (59)$$

Computing integrals in $d\rho$ we get

$$-\frac{16 \kappa_2}{3 \pi \delta_2} \left(\mathbf{n} \cdot \nabla u_2(\mathbf{0}) \right) + \mathcal{O}(1) - \frac{2 \kappa_1}{\delta_2^2} (u_1(\mathbf{0}) - u_2(\mathbf{0})) + \frac{8 \kappa_1}{3 \pi \delta_2} \left(\mathbf{n} \cdot \nabla u_1(\mathbf{0}) \right) + \frac{8 \kappa_2}{3 \pi \delta_1} \left(\mathbf{n} \cdot \nabla u_2(\mathbf{0}) \right) = f. \quad (60)$$

Multiplying the above equation by δ_2^2 we again obtain

$$u_1(\mathbf{x}) = u_2(\mathbf{x}) \quad \text{on } \mathbf{x} \in \Gamma. \quad (61)$$

Therefore, multiplying equation (60) by δ_2 we get

$$-\frac{16\kappa_2}{3\pi}(\mathbf{n} \cdot \nabla u_2(\mathbf{0})) + \mathcal{O}(\delta_2) + \frac{8\kappa_1}{3\pi}(\mathbf{n} \cdot \nabla u_1(\mathbf{0})) + \frac{8\kappa_2\delta_2}{3\pi\delta_1}(\mathbf{n} \cdot \nabla u_2(\mathbf{0})) = \delta_2 f. \quad (62)$$

Taking limits in the above equations provides us with

$$\kappa_1(\mathbf{n} \cdot \nabla u_1(\mathbf{x})) = \kappa_2(\mathbf{n} \cdot \nabla u_2(\mathbf{x})) \quad \text{on } \mathbf{x} \in \Gamma. \quad (63)$$

Therefore the nonlocal interface conditions converge to their local counterpart.

6. Numerical Results

In this section we carry out a preliminary numerical investigation of the NLI theory developed in this paper. To simplify the numerical implementation we consider a one-dimensional interface problem with a slightly different configuration of the domains Ω_1 and Ω_2 ; see Figure 6.

The domains are discretized using an interface-fitted finite element grid \mathcal{T}_h having N_h nodes x_i and $N_h - 1$ elements of size h . We denote the node on the interface by x_{i_Γ} . On each subdomain we approximate the nonlocal solution by a piecewise linear C^0 finite element space endowed with the standard Lagrangian nodal basis φ_i . To allow the nonlocal solution to develop a discontinuity on the interface we “double-count” the degree-of-freedom living on the interface node x_{i_Γ} . Discretization of the nonlocal interface problem results in a $(N_h + 1) \times (N_h + 1)$ linear system of algebraic equations $\mathbf{A}\mathbf{u} = \mathbf{f}$, where

$$\begin{aligned} A_{ij} &= \int_{\Omega \cup \tilde{\Gamma}} \left[\int_{\Omega \cup \tilde{\Gamma}} \gamma(x, y) (\varphi_j(x) - \varphi_j(y)) (\varphi_i(x) - \varphi_i(y)) dy \right] dx, \\ f_i &= \int_{\Omega} f(x) \varphi_i(x) dx, \end{aligned} \quad (64)$$

for $i, j = 1, \dots, i_\Gamma, i_\Gamma, \dots, N_h$. In equation (64), $\Omega = \Omega_1 \cup \Omega_2$, $\tilde{\Gamma} = \Gamma_1 \cup \Gamma_2$. Let κ_1 and κ_2 be two positive constants describing the material properties in Ω_1 and Ω_2 , respectively, and let \mathcal{X}_{B_i} be the characteristic function of the ball $B_i(x) = \{y : |x - y| < \delta_i\}$, with $i = 1, 2$. The kernel in equation (64) is defined as

$$\gamma(x, y) = \begin{cases} \gamma_{11}(x, y) = \frac{3}{2} \frac{\kappa_1}{\delta_1^3} \mathcal{X}_{B_1(x)}(y) & (x, y) \in \{\Omega_1 \cup \Gamma_1 \times \Omega_1 \cup \Gamma_1\} \\ \gamma_{12}(x, y) = C_{12}(\delta_1) \mathcal{X}_{B_1(x)}(y) & (x, y) \in \{\Omega_1 \cup \Gamma_1 \times \Omega_2 \cup \Gamma_2\} \\ \gamma_{21}(x, y) = C_{21}(\delta_2) \mathcal{X}_{B_2(x)}(y) & (x, y) \in \{\Omega_2 \cup \Gamma_2 \times \Omega_1 \cup \Gamma_1\} \\ \gamma_{22}(x, y) = \frac{3}{2} \frac{\kappa_2}{\delta_2^3} \mathcal{X}_{B_2(x)}(y) & (x, y) \in \{\Omega_2 \cup \Gamma_2 \times \Omega_2 \cup \Gamma_2\}, \end{cases} \quad (65)$$

The values of C_{12} and C_{21} necessary to complete the kernel definition (65) require some additional considerations and will be discussed shortly. Let $\kappa_1 = 1$ and $\kappa_2 = 3$ in equation (65) and consider the domains

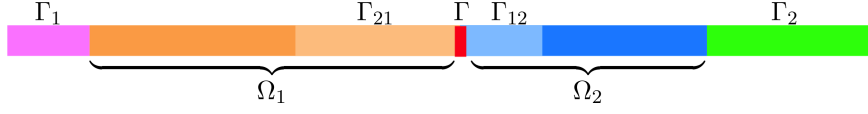


Figure 6: Domains configuration for the numerical results. Note that Γ is a point in this one-dimensional setting.

$\Gamma_1 = [-\delta_1 - 0.5, -0.5]$, $\Omega_1 = (-0.5, 0)$, $\Omega_2 = (0, 0.5)$ and $\Gamma_2 = [0.5, 0.5 + \delta_2]$, so that $\bar{\Omega} \cup \tilde{\Gamma} = [-\delta_1 - 0.5, 0.5 + \delta_2]$. The volume constraints for the nonlocal problem are

$$g_1(x) = \frac{1}{16} - \frac{1}{8}x - \frac{1}{2}x^2, \quad g_2(x) = \frac{1}{16} - \frac{1}{24}x - \frac{1}{6}x^2. \quad (66)$$

The convergence to the local limits, also referred to as δ -convergence, is investigated numerically with progressive reduction of δ_1 and δ_2 , as explained next. Consider the following local interface problem

$$\begin{cases} -\kappa_1 \frac{d^2 u_1}{dx^2}(x) = f_1(x) & \text{in } (-0.5, 0) \\ -\kappa_2 \frac{d^2 u_2}{dx^2}(x) = f_2(x) & \text{in } (0, 0.5) \\ u_1(-0.5) = 0 \\ u_2(0.5) = 0 \\ u_1(0) = u_2(0) \\ \kappa_1 \frac{du_1}{dx}(0) = \kappa_2 \frac{du_2}{dx}(0), \end{cases} \quad (67)$$

with $\kappa_1 = 1$, $\kappa_2 = 3$ and $f_1 = f_2 = 1$. The analytic solution u_L of the above problem is

$$u_L(x) = \begin{cases} u_1(x) = g_1(x) & x \in (-0.5, 0) \\ u_2(x) = g_2(x) & x \in (0, 0.5), \end{cases} \quad (68)$$

where g_1 and g_2 are the volume constraints of the nonlocal problem, defined in equation (66). The right hand side for the nonlocal problem is the same given to the local problem just described. To assess δ -convergence, we fix a value of h associated with a fine enough grid and progressively half δ_1 and δ_2 , as $\|u_{N,h} - u_L\|_{L^2(\Omega \cup \tilde{\Gamma})}$ is monitored, where $u_{N,h}$ is the finite element nonlocal solution associated with a grid of size h and the norm is taken over $\Omega \cup \tilde{\Gamma}$. Note that from now on we drop the dependence of the norms on the domain. For these tests, we consider four different choices of kernels.

Kernel 1:

$$C_{12}(\delta_1) = \frac{3}{2} \frac{\kappa_2}{\delta_1^3}, \quad C_{21}(\delta_2) = \frac{3}{2} \frac{\kappa_1}{\delta_2^3}. \quad (69)$$

Kernel 2:

$$C_{12}(\delta_1) = \frac{3}{2} \frac{\kappa_1}{\delta_1^3}, \quad C_{21}(\delta_2) = \frac{3}{2} \frac{\kappa_2}{\delta_2^3}. \quad (70)$$

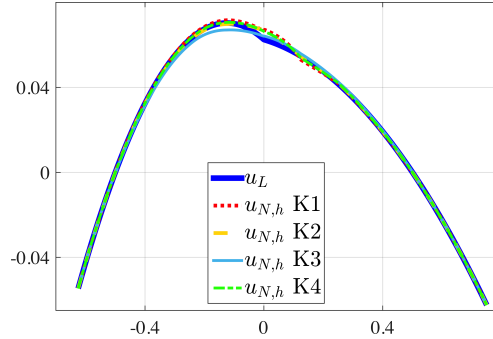


Figure 7: Comparison of nonlocal solution and exact local for different kernels. $\delta_1 = 2^{-3}, \delta_2 = 2^{-2}, h = 2^{-12}$.

Kernel 3:

$$C_{12}(\delta_1) = C_{21}(\delta_2) = \frac{3}{4} \left(\frac{\kappa_1}{\delta_1^3} + \frac{\kappa_2}{\delta_2^3} \right). \quad (71)$$

Kernel 4:

$$C_{12}(\delta_1) = \frac{3}{4} \left(\frac{\kappa_1}{\delta_1^3} + \frac{\kappa_2}{\delta_1^3} \right), \quad C_{21}(\delta_2) = \frac{3}{4} \left(\frac{\kappa_1}{\delta_2^3} + \frac{\kappa_2}{\delta_2^3} \right). \quad (72)$$

The values of C_{11} and C_{22} are defined as in equation (65). Results for all the above kernels are reported in Table 1 considering a mesh of size $h = 2^{-12}$. For such a value of h , the error $\|u_{L,h} - u_L\|_{L^2}$ between the numerical solution $u_{L,h}$ of problem (67) and the analytic solution u_L is of order 10^{-9} , hence we are allowed to use u_L in place of $u_{L,h}$ to monitor the δ -convergence, because the h error is negligible compared to the δ error. Three Gauss points have been used for the assembly procedure and for the norm computation and a double node is present at the interface. From Table 1, we see that the error between the nonlocal and the local solution

δ_1, δ_2	Kernel 1		Kernel 2		Kernel 3		Kernel 4	
	$\ u_{N,h} - u_L\ _{L^2}$	order						
$2^{-5}, 2^{-4}$	1.62e-04	–	3.86e-04	–	7.72e-04	–	2.61e-04	–
$2^{-6}, 2^{-5}$	6.69e-05	1.28	2.19e-04	0.82	4.22e-04	0.87	1.45e-04	0.84
$2^{-7}, 2^{-6}$	3.11e-05	1.11	1.16e-04	0.91	2.20e-04	0.94	7.72e-05	0.91
$2^{-8}, 2^{-7}$	1.52e-05	1.04	6.01e-05	0.95	1.12e-04	0.97	3.98e-05	0.95
$2^{-9}, 2^{-8}$	7.52e-06	1.01	3.05e-05	0.98	5.68e-05	0.98	2.02e-05	0.98
$2^{-10}, 2^{-9}$	3.75e-06	1.00	1.54e-05	0.99	2.86e-05	0.99	1.02e-05	0.99

Table 1: δ convergence in one dimension.

goes to zero with a first order convergence for all kernels, showing how the local model can be recovered from the nonlocal model. Note that the convergence is first order because we are considering an interface problem. It would have been second order for a boundary value problem. In Figure 7, we show the nonlocal solution obtained with the different kernels compared to the local exact u_L , using relatively large values of δ_1 and δ_2 ,

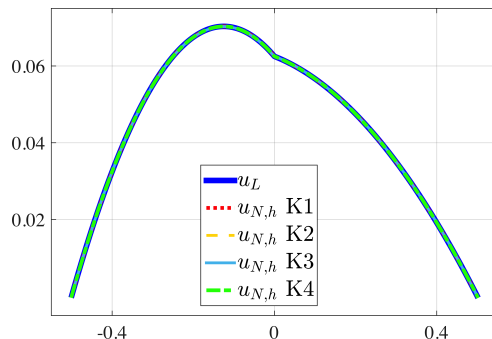


Figure 8: Comparison of nonlocal solution and exact local for different kernels. $\delta_1 = 2^{-10}, \delta_2 = 2^{-9}, h = 2^{-12}$.

namely $\delta_1 = 2^{-3}$ and $\delta_2 = 2^{-2}$. Note that the nonlocal solution obtained using Kernel 3 is the one that differs the most compared to the other nonlocal solutions. The reason for this behavior is that Kernel 3 is the only one among the four that is symmetric across the interface (i.e. $C_{12} = C_{21}$). In Figure 8, we show the nonlocal solution obtained with the different kernels compared to the local exact u_L , using small values of δ_1 and δ_2 , namely $\delta_1 = 2^{-10}$ and $\delta_2 = 2^{-9}$. This figure is meant to give visual proof that all kernels considered provide a nonlocal solution that converges to the local exact as δ_1 and δ_2 approach zero.

To investigate the h -convergence of the proposed finite element approximation, let $u_{N,h_{fine}}$ be a finite element nonlocal solution associated with a grid of size h_{fine} , with $h_{fine} \ll h$. Clearly, if $h_{fine} = h$, then $u_{N,h} = u_{N,h_{fine}}$. For fixed values of δ_1 and δ_2 , the h -convergence is assessed by progressively halving h and monitoring $\|u_{N,h} - u_{N,h_{fine}}\|_{L^2}$. Results are shown in Table 2 for $\delta_1 = 2^{-5}, \delta_2 = 2^{-4}$, and $h_{fine} = 2^{-12}$. Three Gauss points have been used for the assembly procedure and for the norm computation. Recall also that a double node is present at the interface, to allow a discontinuous nonlocal solution. From Table 2, we see that the expected quadratic order of convergence given by the use of linear finite elements is obtained only for Kernel 1, whereas the other kernels display a rapidly deteriorating rate. In light of Table 2, from now on we only consider Kernel 1, given in equation (69). Note also that Kernel 1 is analogous to the one used to obtain the local limits.

	Kernel 1		Kernel 2		Kernel 3		Kernel 4	
h	$\ u_{N,h} - u_{N,h_{fine}}\ _{L^2}$	order						
2^{-5}	6.58e-05	–	5.86e-05	–	5.79e-05	–	6.07e-05	–
2^{-6}	1.63e-05	2.01	1.36e-05	2.10	1.32e-05	2.13	1.44e-05	2.07
2^{-7}	3.94e-06	2.05	3.33e-06	2.03	4.08e-06	1.69	3.43e-06	2.07
2^{-8}	9.49e-07	2.05	1.18e-06	1.45	2.21e-06	0.88	9.39e-07	1.87
2^{-9}	2.33e-07	2.02	6.77e-07	0.80	1.40e-06	0.65	4.25e-07	1.14

Table 2: h -convergence in one dimension.

In Figure 9, a plot of the numerical nonlocal solution for different values of δ_1 and δ_2 is compared to the local solution in equation (68). It can be seen from the pictures that the nonlocal solution has a jump discontinuity at the interface, and that the magnitude of the jump approaches zero as δ_1 and δ_2 approach zero, as proven by the results in Table 1. The behavior of the jump discontinuity at the interface of the nonlocal

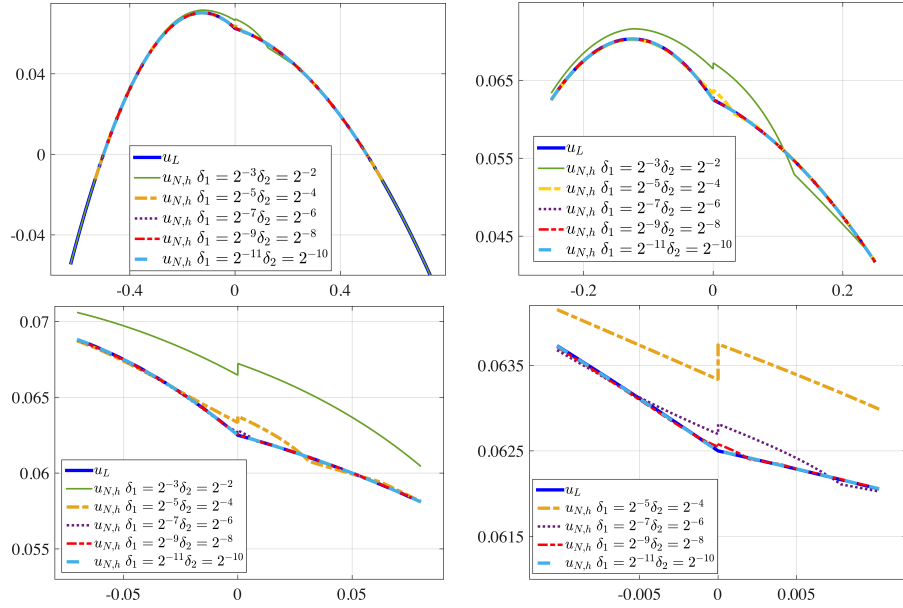


Figure 9: Numerical nonlocal solutions compared to the local exact solution in equation (68). The pictures are progressively zoomed on the interface moving from left to right and from top to bottom.

solution is investigated in Tables 3 and 4. The magnitude of the jump is computed as the difference of the solution values at the double node that has been placed at the interface. In Table 3, we consider $\delta_1 = 2^{-5}$, $\delta_2 = 2^{-4}$, $\kappa_1 = 1$, and $\kappa_2 = 3$ as h is decreased. As expected, the magnitude of the discontinuity reaches a saturation value. This behavior is due to the fact that the discontinuity is associated with the values of $\delta_1 = 2^{-5}$, $\delta_2 = 2^{-4}$ which define the nonlocal solution. On the other hand, in Table 4, we fix $h = 2^{-12}$, $\kappa_1 = 1$,

$\delta_1 = 2^{-5}, \delta_2 = 2^{-4}, \kappa_1 = 1, \kappa_2 = 3$		
h	discontinuity magnitude	order
2^{-5}	6.50e-04	—
2^{-6}	4.23e-04	0.62
2^{-7}	4.17e-04	1.99e-02
2^{-8}	4.15e-04	6.20e-03
2^{-9}	4.15e-04	1.00e-04
2^{-10}	4.15e-04	3.00e-04
2^{-11}	4.15e-04	0.00

Table 3: Magnitude of the jump discontinuity at the interface of the nonlocal solution, for fixed δ_1 and δ_2 and decreasing h .

and $\kappa_2 = 3$ and progressively half δ_1 and δ_2 . The result is that the magnitude of the discontinuity goes to zero with approximately first order convergence. This shows that the nonlocal solution starts as discontinuous, and as it converges to the local solution becomes continuous. To complete this one-dimensional investigation, we

$h = 2^{-12}, \kappa_1 = 1, \kappa_2 = 3,$		
δ	discontinuity magnitude	order
$\delta_1 = 2^{-5}, \delta_2 = 2^{-4}$	4.15e-04	—
$\delta_1 = 2^{-6}, \delta_2 = 2^{-5}$	2.25e-04	0.88
$\delta_1 = 2^{-7}, \delta_2 = 2^{-6}$	1.17e-04	0.94
$\delta_1 = 2^{-8}, \delta_2 = 2^{-7}$	5.95e-05	0.97
$\delta_1 = 2^{-9}, \delta_2 = 2^{-8}$	3.00e-05	0.99
$\delta_1 = 2^{-10}, \delta_2 = 2^{-9}$	1.51e-05	0.99

Table 4: Magnitude of the jump discontinuity at the interface of the nonlocal solution, for fixed h and decreasing δ_1 and δ_2 .

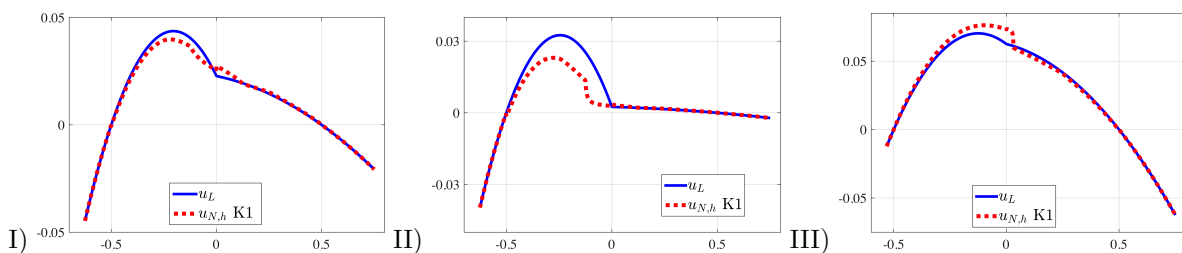


Figure 10: Nonlocal solution for $h = 2^{-12}$ and: I) $\kappa_1 = 1, \kappa_2 = 10, \delta_1 = 2^{-3},$ and $\delta_2 = 2^{-2}$. II) $\kappa_1 = 1, \kappa_2 = 100, \delta_1 = 2^{-3},$ and $\delta_2 = 2^{-2}$. III) $\kappa_1 = 1, \kappa_2 = 3, \delta_1 = 2^{-5},$ and $\delta_2 = 2^{-2}$.

also report pictures of nonlocal solutions obtained with a larger difference between the values of κ_1 and κ_2 , or between the values of δ_1 and δ_2 , see Figure 10.

Acknowledgments

This work was supported by the Sandia National Laboratories (SNL) Laboratory-directed Research and Development (LDRD) program, and the U.S. Department of Energy, Office of Science, Office of Advanced Scientific Computing Research under Award Number DE-SC-0000230927 and under the Collaboratory on Mathematics and Physics-Informed Learning Machines for Multiscale and Multiphysics Problems (PhILMs) project. SNL is a multimission laboratory managed and operated by National Technology and Engineering Solutions of Sandia, LLC., a wholly owned subsidiary of Honeywell International, Inc., for the U.S. Department of Energy's National Nuclear Security Administration under contract DE-NA-0003525.

This paper describes objective technical results and analysis. Any subjective views or opinions that might be expressed in the paper do not necessarily represent the views of the U.S. Department of Energy or the United States Government. Report number SAND2020-0270.

In memoriam

This paper is dedicated to the memory of Dr. Douglas Nelson Woods (January 11 1985 - September 11 2019), promising young scientist and post-doctoral research fellow at Los Alamos National Laboratory. Our thoughts and wishes go to his wife Jessica, to his parents Susan and Tom, to his sister Rebecca and to his brother Chris, whom he left behind.

References

- [1] D. A. Benson, S. W. Wheatcraft, M. M. Meerschaert, Application of a fractional advection-dispersion equation, *Water resources research* 36 (6) (2000) 1403–1412.
- [2] R. Schumer, D. A. Benson, M. M. Meerschaert, S. W. Wheatcraft, Eulerian derivation of the fractional advection–dispersion equation, *Journal of contaminant hydrology* 48 (1-2) (2001) 69–88.
- [3] R. Schumer, D. A. Benson, M. M. Meerschaert, B. Baeumer, Multiscale fractional advection-dispersion equations and their solutions, *Water Resources Research* 39 (1).
- [4] A. H. Delgosaie, D. W. Meyer, P. Jenny, H. A. Tchelepi, Non-local formulation for multiscale flow in porous media, *Journal of Hydrology* 531 (2015) 649–654.
- [5] S. A. Silling, Reformulation of elasticity theory for discontinuities and long-range forces, *Journal of the Mechanics and Physics of Solids* 48 (1) (2000) 175–209.
- [6] Y. D. Ha, F. Bobaru, Characteristics of dynamic brittle fracture captured with peridynamics, *Engineering Fracture Mechanics* 78 (6) (2011) 1156–1168.
- [7] D. J. Littlewood, Simulation of dynamic fracture using peridynamics, finite element modeling, and contact, in: *Proceedings of the ASME 2010 International Mechanical Engineering Congress and Exposition (IMECE)*, 2010, pp. 209–217.
- [8] A. Buades, B. Coll, J.-M. Morel, Image denoising methods. a new nonlocal principle, *SIAM review* 52 (1) (2010) 113–147.
- [9] G. Gilboa, S. Osher, Nonlocal linear image regularization and supervised segmentation, *Multiscale Modeling & Simulation* 6 (2) (2007) 595–630.
- [10] G. Gilboa, S. Osher, Nonlocal operators with applications to image processing, *Multiscale Modeling & Simulation* 7 (3) (2008) 1005–1028.
- [11] Y. Lou, X. Zhang, S. Osher, A. Bertozzi, Image recovery via nonlocal operators, *Journal of Scientific Computing* 42 (2) (2010) 185–197.
- [12] A. A. Schekochihin, S. C. Cowley, T. A. Yousef, MHD turbulence: Nonlocal, anisotropic, nonuniversal?, in: *IUTAM Symposium on computational physics and new perspectives in turbulence*, Springer, 2008, pp. 347–354.
- [13] E. Askari, F. Bobaru, R. Lehoucq, M. Parks, S. Silling, O. Weckner, Peridynamics for multiscale materials modeling, in: *Journal of Physics: Conference Series*, Vol. 125, IOP Publishing, 2008, p. 012078.
- [14] B. Alali, R. Lipton, Multiscale dynamics of heterogeneous media in the peridynamic formulation, *Journal of Elasticity* 106 (1) (2012) 71–103.
- [15] P. W. Bates, A. Chmaj, An integrodifferential model for phase transitions: stationary solutions in higher space dimensions, *Journal of statistical physics* 95 (5-6) (1999) 1119–1139.
- [16] P. Fife, Some nonclassical trends in parabolic and parabolic-like evolutions, in: *Trends in nonlinear analysis*, Springer, 2003, pp. 153–191.

- [17] M. M. Meerschaert, A. Sikorskii, Stochastic models for fractional calculus, Vol. 43, Walter de Gruyter, 2011.
- [18] M. D’Elia, Q. Du, M. Gunzburger, R. Lehoucq, Nonlocal convection-diffusion problems on bounded domains and finite-range jump processes, Computational Methods in Applied Mathematics 17 (4) (2017) 707–722.
- [19] N. Burch, M. D’Elia, R. B. Lehoucq, The exit-time problem for a Markov jump process, The European Physical Journal Special Topics 223 (14) (2014) 3257–3271.
- [20] B. Alali, M. Gunzburger, Peridynamics and material interfaces, Journal of Elasticity 120 (2) (2015) 225–248.
- [21] P. Seleson, M. Gunzburger, M. L. Parks, Interface problems in nonlocal diffusion and sharp transitions between local and nonlocal domains, Computer Methods in Applied Mechanics and Engineering 266 (2013) 185–204.
- [22] A. Javili, S. Kaessmair, P. Steinmann, General imperfect interfaces, Computer Methods in Applied Mechanics and Engineering 275 (2014) 76 – 97.
- [23] Q. Du, M. Gunzburger, R. B. Lehoucq, K. Zhou, A nonlocal vector calculus, nonlocal volume-constrained problems, and nonlocal balance laws, Mathematical Models and Methods in Applied Sciences 23 (03) (2013) 493–540.